Dalton Transactions

Accepted Manuscript

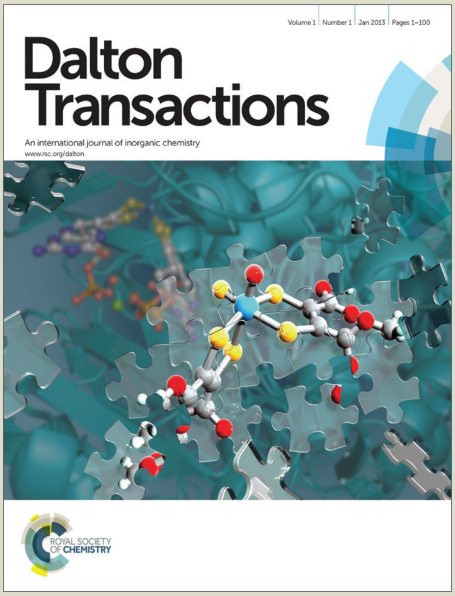

This is an *Accepted Manuscript*, which has been through the Royal Society of Chemistry peer review process and has been accepted for publication.

Accepted Manuscripts are published online shortly after acceptance, before technical editing, formatting and proof reading. Using this free service, authors can make their results available to the community, in citable form, before we publish the edited article. We will replace this *Accepted Manuscript* with the edited and formatted *Advance Article* as soon as it is available.

You can find more information about *Accepted Manuscripts* in the Information for Authors.

Please note that technical editing may introduce minor changes to the text and/or graphics, which may alter content. The journal's standard Terms & Conditions and the Ethical guidelines still apply. In no event shall the Royal Society of Chemistry be held responsible for any errors or omissions in this *Accepted Manuscript* or any consequences arising from the use of any information it contains.

ROYAL SOCIETY OF CHEMISTRY

www.rsc.org/dalton

Cite this: DOI: 10.1039/c0xx00000x

www.rsc.org/xxxxxx

ARTICLE TYPE

Designed synthesis of a series of zwitterion-polyoxometalate hybrid materials for selective scavenging and photolysis of dyes

Sha Ou,[a] Jun-Ping Zheng,[a] Guo-Qiang Kong[a] and Chuan-De Wu*[a]

Received (in XXX, XXX) Xth XXXXXXXXX 20XX, Accepted Xth XXXXXXXXX 20XX
DOI: 10.1039/b000000x

Zwitterions and polyoxometalates (POMs) are two kinds of functional moieties with very different properties for applications in different fields. We have developed an effective strategy to successfully immobilize these two different zwitterion and POM moieties into the frameworks of porous hybrid materials, in which the POM units act as templates and photoactive moieties. These hybrid materials demonstrate remarkable efficiency on selective scavenging and photolysis of cationic dyes from polluted water, in which up to 10% dye uptake and quantitative photolysis of dyes have been realized.

Introduction

In the past decades, rational design and synthesis of metal-organic frameworks (MOFs) have achieved great progress that is driven by their fascinating topological architectures and interesting properties for potential applications in the fields of nonlinear optics (NLO),[1] catalysis,[2] luminescence,[3] magnetism,[4] separation,[5] gas storage[6] and molecular sensing.[7]

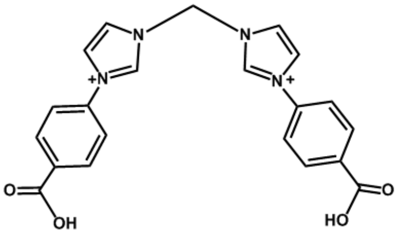

Scheme 1 1,1'-methylenebis(3-(4-carboxyphenyl)-1H-imidazol-3-ium) (H_2**L**) ligand.

Zwitterionic complexes are a class of functional moieties which have been used as ionic liquid precursors or ionic liquids for a number of applications, such as cleaner and green and environmentally friendly reaction media.[8] Due to their flexible coordination ability and structural configurations, introducing zwitterionic moieties into porous MOFs may result in some interesting materials with special properties for applications in different fields.[9] However, controlled by their zwitterionic nature and flexible backbones, it is very difficult to synthesize highly stable and porous MOF materials, whereas the porosity is an essential element for their divers applications. Therefore, the synthesis strategy for zwitterion-based metal-organic coordination networks has to be developed. Considering that polyoxometalates (POMs) have nanosized dimensions and redox chemistry, photochemistry and charge distribution properties,[10-12] our strategy is using POMs as the templates and the secondary functional moieties to direct the formation of porous zwitterion-POM composite materials. Herein we report a series of porous zwitterion-POM hybrid materials based on a zwitterionic ligand (1,1'-methylenebis(3-(4-carboxyphenyl)-1H-imidazol-3-ium) = H_2**L**; Scheme 1) containing two charged aromatic azolium components connected with zinc(II) ions, and templated by Keggin-type POM polyanions. These hybrid materials demonstrate interesting properties in selective scavenging and photolysis of dyes from water solutions.

Experimental Section

Materials and Measurements. All of the chemicals were obtained from commercial sources and were used without further purification, except 1,1'-methylenebis(3-(4-carboxyphenyl)-1H-imidazol-3-ium) chloride (H_2**L**Cl_2) was prepared according to the literature.[13] Elemental analyses were performed on a ThermoFinnigan Flash EA 1112 elementary analyzer. FT-IR spectra were recorded from KBr pellets on a FTS-40 spectrophotometer in the 4000-400 cm^{-1} region. Thermogravimetric analyses (TGA) were carried out on a SDTQ600 compositional analysis instrument from 30 to 800 °C under N_2 atmosphere at a heating rate of 10 °C min^{-1}. Powder X-ray diffraction data (PXRD) were recorded on a RIGAKU D/MAX 2550/PC for Cu-Kα (λ = 1.5406 Å). Luminescence spectra of the solid samples were recorded on a Hitachi F4600 fluorescence spectrometer at room temperature. ^{1}H NMR and ^{13}C NMR spectra were recorded on a 400 MHz spectrometer in DMSO solution and the chemical shifts were reported relative to internal standard TMS (0 ppm).

Synthesis of H_2L$(PF_6)_2$. KPF_6 (1.47 g, 8 mmol) was added to H_2**L**Cl_2 (2.0 g, 3.6 mmol) in 20 mL distilled H_2O, and the mixture was stirred at room temperature for 12 h. The resulting solid was collected by filtration, washed with water, and dried at 65 °C (Yield: 98%). ^{1}H NMR (400 MHz, DMSO): δ = 6.83 (s, 2H), 7.92 (m, 4H), 8.27 (t, 6H), 8.51 (d, 2H), 10.16 (s, 2H). ^{13}C NMR (100 MHz, DMSO): δ = 59.0, 121.7, 122.1, 123.2, 131.3, 132.4,

Dalton Transactions Accepted Manuscript

137.4, 137.7, 166.1. IR (KBr pellet, ν/cm^{-1}): 1702(s), 1611(m), 1552(s), 1433(m), 1388(m), 1334(w), 1316(w), 1288(m), 1212(m), 1119(m), 1075(m), 1020(w), 958(w), 848(s), 771(m), 740(m), 691(m), 677(m), 626(w), 617(w), 522(m).

Synthesis of [ZnLCl$_2$]·H$_2$O (1). A mixture of H$_2$**L**Cl$_2$ (15 mg, 0.02 mmol) and Zn(NO$_3$)$_2$·6H$_2$O (30 mg, 0.1 mmol) in a mixed solvent of 0.2 mL diluted hydrochloric acid (pH = 1), 10 mL H$_2$O and 10 mL DMF was heated at 80 °C for five days. Colorless crystals of **1** were isolated by filtration, washed with MeOH, and dried in air (Yield: 56%). Anal. Cald. for $C_{21}H_{18}ZnN_4O_5Cl_2$ (%): C, 46.48; H, 3.34; N, 10.32. Found (%): C, 46.65; H, 3.42; N, 10.31. IR (KBr pellet, ν/cm^{-1}): 1625(s), 1561(m), 1550(m), 1384(s), 1355(s), 1205(s), 1069(w), 1015(w), 864(w), 834(w), 781(m), 736(w), 700(m), 629(w), 522(w).

Synthesis of [(CH$_3$)$_2$NH$_2$][ZnL$_2$(PW$_{12}$O$_{40}$)]·8DMF·14H$_2$O (2). H$_2$**L**(PF$_6$)$_2$ (15 mg, 0.02 mmol), Na$_3$PW$_{12}$O$_{40}$ (67 mg, 0.02 mmol) and Zn(NO$_3$)$_2$·6H$_2$O (30 mg, 0.1 mmol) were thoroughly dissolved in 10 mL H$_2$O and 10 mL DMF. The mixture was heated at 80 °C for one day. Colorless crystals of **2** were isolated by filtration, washed with H$_2$O and EtOH, and dried in air (Yield: 85%). Anal. Cald. for $C_{68}H_{132}ZnN_{17}O_{70}PW_{12}$ (%): C, 17.72; H, 2.89; N, 5.16. Found (%): C, 17.78; H, 2.83; N, 5.17. IR (KBr pellet, ν/cm^{-1}): 1618(s), 1553(s), 1382(s), 1212(s), 1087(m), 1052(m), 1013(w), 950(s), 888(m), 811(s), 834(w), 784(w), 716(m), 621(w), 519(m).

Synthesis of [(CH$_3$)$_2$NH$_2$]$_2$[ZnL$_2$(SiW$_{12}$O$_{40}$)]·7DMF·13H$_2$O (3). The synthesis procedure of **3** is similar to that of **2**, except Na$_3$PW$_{12}$O$_{40}$ was replaced by Na$_4$SiW$_{12}$O$_{40}$ (Yield: 43%). Anal. Cald. for $C_{67}H_{130}ZnN_{17}O_{68}SiW_{12}$ (%): C, 17.64; H, 2.87; N, 5.22. Found (%): C, 17.60; H, 2.89; N, 5.21. IR (KBr pellet, ν/cm^{-1}): 1617(s), 1552(s), 1382(s), 1212(s), 1072(m), 1013(w), 995(m), 945(s), 896(s), 785(s), 703(s), 625(w), 525(m).

Synthesis of [(CH$_3$)$_2$NH$_2$]$_3$[ZnL$_2$(BW$_{12}$O$_{40}$)]·4DMF·4H$_2$O (4). The synthesis procedure of **4** is similar to that of **2**, except Na$_3$PW$_{12}$O$_{40}$ was replaced by K$_5$BW$_{12}$O$_{40}$ (Yield: 66%). Anal. Cald. for $C_{60}H_{96}ZnN_{15}O_{56}BW_{12}$ (%): C, 17.13; H, 2.30; N, 5.00. Found (%): C, 17.17; H, 2.31; N, 5.03. IR (KBr pellet, ν/cm^{-1}): 1618(s), 1550(s), 1378(s), 1213(s), 1118(m), 1071(m), 1017(w), 934(s), 876(s), 761(s), 614(w), 452(m).

Synthesis of [(CH$_3$)$_2$NH$_2$]$_4$[ZnL$_2$(CoW$_{12}$O$_{40}$)]·4DMF·7H$_2$O (5). The synthesis procedure of **5** is similar to that of **2**, except Na$_3$PW$_{12}$O$_{40}$ was replaced by K$_6$CoW$_{12}$O$_{40}$ (Yield: 63%). Anal. Cald. for $C_{62}H_{110}N_{16}O_{59}CoW_{12}Zn$ (%): C, 17.10; H, 2.55; N, 5.15. Found (%): C, 17.13; H, 2.50; N, 5.14. IR (KBr pellet, ν/cm^{-1}): 1617(s), 1560(w), 1548(s), 1383(s), 1330(w), 1309(w), 1211(s), 1108(m), 1071(m), 1016(w), 934(s), 876(s), 762(s), 615(m), 453(m).

A typical procedure for the dye adsorption experiments. A solid sample (3 mg) was added to 3 mL aqueous solution of dye (100 mg·L^{-1}) under stirring at room temperature, which was further stirred at room temperature for 24 h. The mixture was centrifugated, and the plasma was analyzed by UV-Vis absorption spectroscopy. The amount of adsorbed dye was calculated from the following mass balance equation:

$$Q_{ad} = \frac{(C_0 - C_{ad})}{m} V$$

where Q_{ad} (mg g^{-1}) is the amount of adsorbed dye by adsorbent, C_0 is the initial concentration of dye in water (mg L^{-1}), C_{ad} is the concentration of dye after adsorption (mg L^{-1}), V is the volume of the solution (L), and m is the mass of adsorbent (g).

Table 1 Crystal data and structure refinements for compounds **1**- **5**.

Compound	**1**	**2**	**3**	**4**	**5**
Chemical formula	$C_{21}H_{18}ZnN_4O_5Cl_2$	$C_{68}H_{132}ZnN_{17}O_{70}PW_{12}$	$C_{67}H_{130}ZnN_{17}O_{68}SiW_{12}$	$C_{60}H_{96}ZnN_{15}O_{56}BW_{12}$	$C_{62}H_{110}ZnN_{16}O_{59}CoW_{12}$
Formula Mass	541.99	4612.05	4558.04	4202.86	4355.89
Crystal system	Orthorhombic	Monoclinic	Monoclinic	Monoclinic	Monoclinic
Space group	*P*nma	*C*2/c	*C*2/c	*C*2/c	*C*2/c
a (Å)	14.5366(10)	21.205(2)	21.826 (18)	20.949(12)	21.018(4)
b (Å)	18.2023(12)	30.853(2)	30.504(16)	31.1225(14)	30.814(5)
c (Å)	8.0806(6)	19.6747(16)	19.495(11)	19.7567(14)	19.639(3)
β (°)	90	100.033(8)	100.29(3)	99.761(15)	99.919(15)
V (Å^3)	2138.1(3)	12675.0(18)	12771(14)	12695(8)	12529(4)
Z	4	4	4	4	4
ρ (g·cm^{-3})	1.686	1.949	1.933	1.935	1.987
μ (mm^{-1})	1.442	11.099	11.012	11.069	11.343
F (000)	1104	6628	6624	6588	6676
data/parameters	2251/157	11217/514	11297/490	10464/484	9456/466
R_{int}	0.0375	0.0494	0.0708	0.0557	0.0658
S	1.020	1.106	1.187	1.042	1.012
R_1, wR_2 ($I>2\sigma(I)$)	0.0758, 0.1744	0.0848, 0.2025	0.0939, 0.2163	0.0843, 0.1835	0.0881, 0.1826
R_1, wR_2 (all data)	0.1105, 0.1961	0.1544, 0.2220	0.1635, 0.2386	0.1548, 0.2027	0.1850, 0.2092

[a] $R_1 = \sum(|F_o| - |F_c|)/\sum|F_o|$, $wR_2 = [\sum[w(F_o^2 - F_c^2)^2]/\sum w(F_o^2)^2]^{0.5}$.

A typical procedure for photolysis of dyes. Methylene blue (MB) aqueous solution (40 mL, 10.0 mg L^{-1}) and compound **2** (30 mg) were stirred at room temperature for 30 min until the adsorption-desorption equilibrium was reached. The mixture was irradiated under a 300 W Xe lamp with a λ≤ 400 nm light cut off filter. The aliquots were regularly taken out for UV-Vis

Dalton Transactions Accepted Manuscript

absorption spectroscopy analysis to determine the decomposition ratio of dye in water by monitoring the maximum absorption peak of MB.

X-ray crystal data collections and structure determinations. The determinations of the unit cells and data collections for the crystals of compounds **1-5** were performed on an Oxford Xcalibur Gemini Ultra diffractometer with an Atlas detector. The data were collected using graphite–monochromatic Mo-Kα radiation (λ = 0.71073 Å) at 293 K. The data sets were corrected by empirical absorption correction using spherical harmonics, implemented in the SCALE3 ABSPACK scaling algorithm.[14] The structures of compounds **1-5** were solved by direct methods and refined by full-matrix least-square methods with the SHELX-97 program package.[15] Because the solvent molecules and counter ions in compounds **2-5** are highly disordered, the SQUEEZE subroutine of the PLATON software suits was used to remove the scattering from the highly disordered guest molecules.[16] The resulting new files were used to further refine the structures. All non-hydrogen atoms were located successfully from Fourier maps. H atoms were generated geometrically. The data collection parameters, crystallographic data, and final agreement factors are collected in Table 1.

Results and Discussion

The reaction between H_2**L**Cl_2 and zinc nitrate in acidified DMF and water at 80 °C resulted in colorless crystals of [Zn**L**Cl_2]·H_2O (**1**). Single crystal X-ray diffraction analysis revealed that compound **1** crystallizes in the orthorhombic *P*nma space group. The fundamental unit of **1** consists of one Zn^{II} cation, two **L** ligands and two chloride anions. The Zn^{II} center adopts tetrahedral coordination environment to coordinate with two monodentate carboxyl groups (Zn-O = 1.970(5) Å) from two **L** ligands and two chloride ions (Zn-Cl = 2.260(3)-2.279(3) Å). The **L** ligand bidentately connects with two Zn(II) centers to extend into a 1D zigzag chain (Fig. 1). TGA chart of **1** shows a weight loss of 3.22 % occurred between 30 and 233 °C, corresponding to the loss of water molecules (expected 3.32 %). There is almost no further weight loss up to 283 °C. Above 283 °C, compound **1** began to lose **L** ligand to decompose.

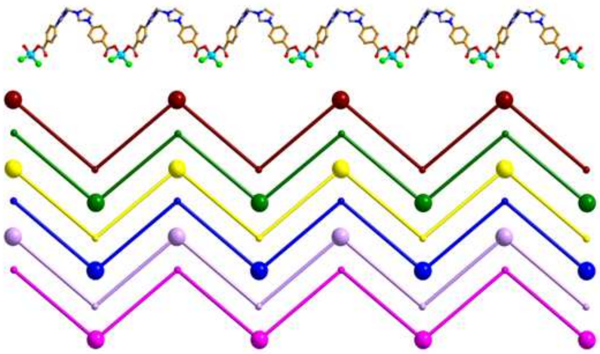

Fig. 1 Ball-and-stick and scheme representations of the zigzag linear network in **1**.

Because of the neutral nature of **L** ligand, there are two chloride ions that occupy two coordination sites of the zinc ion to balance the electric charge in **1**, which cut off the way to extend the connection of the building synthons for the formation of high dimensional porous coordination network. Therefore, if the chloride anions are replaced with suitable anions, such as POMs, during the crystal formation process, high dimensional porous materials might be generated. To facilitate the substitution, chloride ions were firstly exchanged with PF_6^- anions, in consideration of the PF_6^- anion that has weak coordination ability with zinc ion. When H_2**L**$(PF_6)_2$, $[XW_{12}O_{40}]^{n-}$ (X = P^V, Si^{IV}, B^{III} and Co^{II}) and $Zn(NO_3)_2 \cdot 6H_2O$ were reacted in DMF and water at 80 °C for one day, four isomorphous porous organic-inorganic hybrid materials $[(CH_3)_2NH_2]_n[ZnL_2(XW_{12}O_{40})]$·guest (**2**, n = 1 and X = P^V; **3**, n = 2 and X = Si^{IV}, **4**, n = 3 and X = B^{III}; **5**, n = 4 and X = Co^{II}**)** were successfully isolated, in which the Keggin-type polyanions $\{XW_{12}O_{40}\}$ act as anionic templates that are incorporated in the structures of these hybrid materials. These compounds are insoluble in water and common organic solvents, such as MeOH, EtOH, THF and DMF. All of the typical vibration bands of the building moieties in compounds **2–5** are clearly visible in the IR spectra (Fig. S8). The formulae of compounds **2-5** were established on the basis of single crystal structures, elemental analyses and TGA results (Figs. S2-S5). The purities of the bulky as-synthesized samples were confirmed by comparison of the simulated PXRD patterns from single crystal structures with the observed experimental PXRD patterns (Fig. S10).

Single crystal X-ray diffraction analysis revealed that compounds **2-5** are isomorphous, which crystallize in the monoclinic *C*2/c space group. Herein we only discuss the crystal structure of compound **2** in detail. The $\{PW_{12}O_{40}\}$ polyoxoanion possesses the well known Keggin-type structure, and all of the bond lengths and angles are consistent with those described in the literature.[17] Because $\{PW_{12}O_{40}\}$ polyoxoanion does not coordinate with Zn^{II} center, the four coordination sites of tetrahedrally coordinated Zn^{II} cation are occupied by four monodentate carboxyl groups from four **L** ligands. As shown in Fig. 2, it is interesting that the four branched zinc centers are bridged by bidentate **L** ligands to form 2D wave-like polymeric lattices with approximate cavity dimensions of 18.7 × 18.7 $Å^2$. Moreover, templated by the $\{PW_{12}O_{40}\}$ polyoxoanions, the wave-like layers are packed in …ABAB… fashion to result in hexagonal-shaped nanotubular channels propagated along the *c* axis, in which the $\{PW_{12}O_{40}\}$ polyoxoanions locate between the gaps of the lamellar networks. The diameter of the 1D channels is approximate 1.5 nm (taking into account the van der Waals radii), in which the vacancies are filled with counter cations, DMF and water molecules. PLATON calculations indicate that the vacant space in **2** is about 52.9% of the crystal volume (6704.9 $Å^3$ of the 12675.1 $Å^3$ unit cell volume).[18] As shown in the TGA curve of **2**, a weight loss of 14.8% occurred between 30-370 °C, corresponding to the release of lattice H_2O, DMF molecules and $[(CH_3)_2NH_2]^+$ cations.

The photoluminescence spectra of the powder samples of compounds **1-5** were measured at room temperature in the solid state upon excitation at 370 nm. As shown in Fig. 3, the luminescent emission peak of compound **1** red-shifts to 453 nm compared with that of the corresponding free H_2**L** ligand (λ_{em} = 444 nm), which is attributed to the intraligand π^*–π or π^*–n

Dalton Transactions Accepted Manuscript

transitions. It is interesting the luminescence intensity is significantly enhanced, which might be arisen from the coordination of **L** ligand to metal cations that could decrease the loss of the energy by radiationless decay of the intraligand emission excited state.[19] However, the emission of compounds **2-5** is almost quenched in the luminescence spectra. These results indicate that some energy transformations might occur between the excited state of **L** ligand and the polyoxoanion $\{XW_{12}O_{40}\}$, which suggest that hybrids **2-5** might have the potential for photocatalysis application.

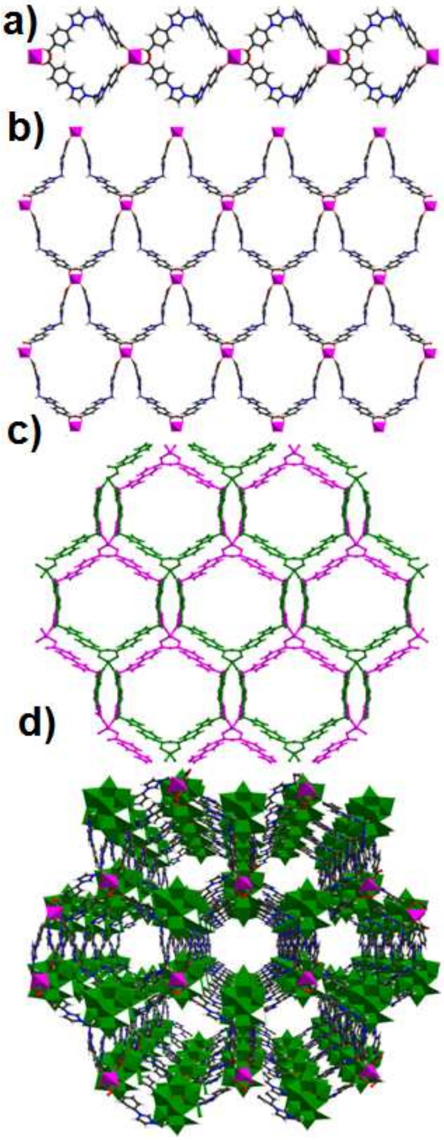

Fig. 2 (a) Side and (b) top views of the 2D diamondoid lamellar network in **2**; (c) A view of the …ABAB… stacked 2D lattices in **2** down the *c* axis; (d) Perspective view of packing diagram of **2** down the *c* axis, showing the 1D opening channels (Color Scheme: Zn, pink tetrahedra; W, green octahedra; P, purple; C, deep grey; H, light grey; N, blue; O, red).

Because dyes are widely used as pigments in textile, paper, printing and plastics industries, the removal of dyes from industrial wastewater by either directed adsorption or photolysis has attracted great attention accompanying the increase of the green environmental consciousness.[20] It is interesting that compounds **2-5** contain two kinds of functional groups of zwitterion and POM moieties, and the anionic charge of these hybrid materials are tunable by changing the Keggin-type $\{XW_{12}O_{40}\}$ polyanions. The remarkable features of these hybrids encouraged us to evaluate the captured ability of different dye molecules. Therefore, the as-synthesized hybrid materials were immersed in different dye aqueous solutions, and the absorbed dyes were quantitatively determined by UV-Vis spectroscopy. Hybrids **2-5** exhibit interesting selective adsorption properties for different dyes that are dependent on the electronic charges. Due to the anionic nature of these hybrid materials, the cationic dyes of methylene blue (MB) and crystal violet (CV) can be fully scavenged from their water solutions with the dye uptakes of 10 and 9.9 wt%, respectively (Fig. 4). However, the adsorption of the anionic dyes of methyl orange (MO) and Conge red (CR) is neglectable, while only trace neutral dye of neutral red (NR) was adsorbed by these adsorbents (Fig. S11). Due to the nonporous nature of compound **1**, only small amount of different dyes were adsorbed. The relative high capture capability of compound **1** in adsorption of anionic MO and CR should be attributed to the abundant cationic moieties in **L** ligands on the solid surfaces (Fig. 5). These results indicate that hybrids **2-5** have great potential for separation of differently charged dyes from their mixtures.

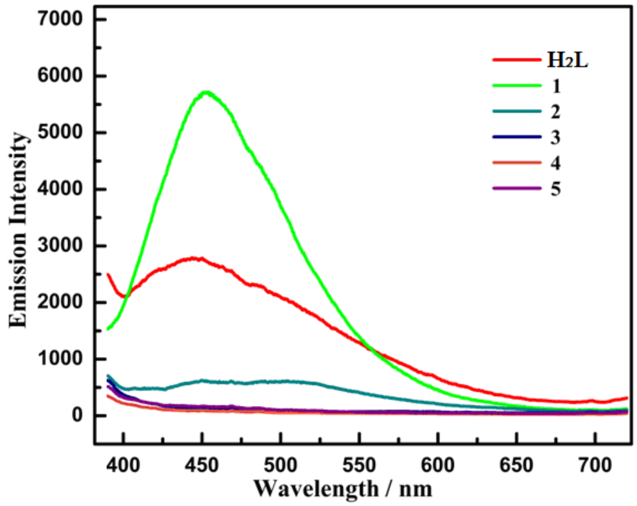

Fig. 3 Luminescence spectra of compounds **1-5** and H_2**L** in the solid-state upon excitation at 370 nm.

The photocatalytic activities of compounds **1-5** were evaluated by degradation of MB, CV, MO and NR dyes (10 mg L^{-1}) in water irradiated under a 300 W Xe lamp in the presence of a $\leq$ 400 nm light cut off filter. The degradation ratios of MB, CV, MO and NR dyes in water were monitored by UV-Vis absorption spectroscopy. As shown in Fig. 6a, the UV-Vis absorption peak of MB dye is quickly disappeared after 17 min in the presence of compound **2** irradiated under a 300 W Xe lamp. No new absorption band was generated in the UV-Vis absorption spectrum, indicating the total decomposition of MB in water.[21] To make a comparison, we further studied the catalytic property of **2** without light irradiation. The UV-Vis absorption spectroscopy analysis demonstrates that the concentration of MB dye in water is slightly decreased, which should be attributed to the adsorption of MB dye by the pores in **2**. As shown in Fig. 6b, compounds **3-**

This journal is © The Royal Society of Chemistry [year]

Dalton Transactions Accepted Manuscript

5 are also highly efficient for the degradation of MB dye under the identical conditions, while compound **1** cannot efficiently degrade MB dye. Due to the cationic nature of CV dye, it can also be easily degraded by compounds **2-5** under otherwise identical conditions (Fig. 7). We further studied the photocatalytic properties of compound **2** toward neutral NR and anionic MO dyes. As shown in Fig. 8, the degradation rate of neutral NR dye is significantly decreased, whereas the degradation rate of anionic MO dye is neglectable (Fig. S15). This is because the affinity between the anionic framework of compound **2** and neutral NR dye is very weak whereas the interaction between compound **2** and anionic MO dye is electrostatic repulsion.

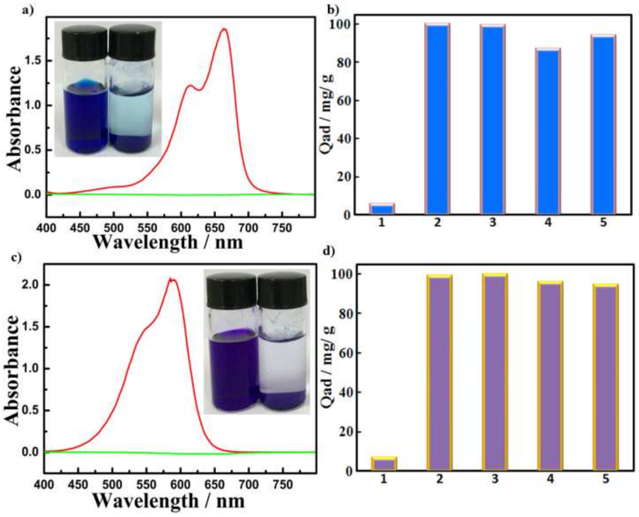

Fig. 4 (a) UV-Vis absorption spectra of MB before (red line) and after (green line) addition of **2** (the inserted pictures highlight the scavenging effect); (b) MB capture capacities of **1-5**; (c) UV-Vis absorption spectra of CV before (red line) and after (green line) addition of **2** (the inserted pictures highlight the scavenging effect); (d) CV capture capacities of **1-5**.

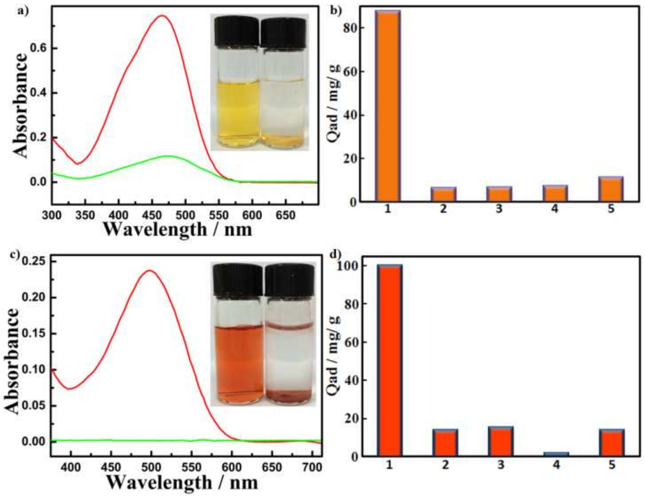

Fig. 5 (a) UV-Vis spectra of MO before (red line) and after (green line) addition of **1** (the inserted pictures highlight the scavenging effect); (b) MO capture capacities of **1-5**; (c) UV-Vis spectra of CR before (red line) and after (green line) addition of **1** (the inserted pictures highlight the scavenging effect); (d) CR capture capacities of **1-5**.

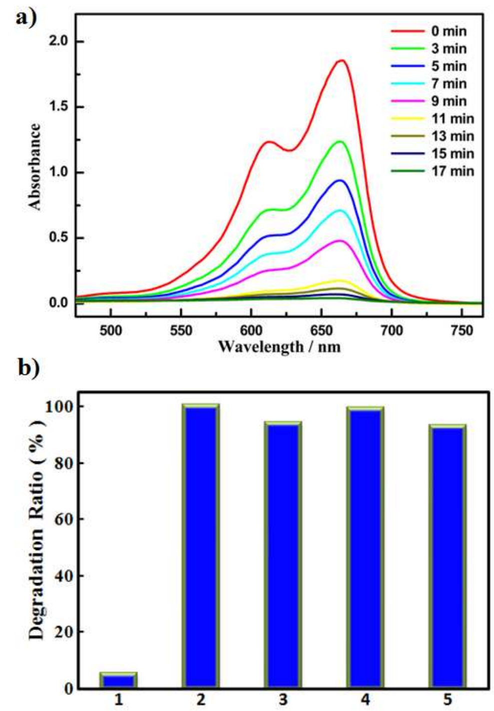

Fig. 6 (a) UV-Vis absorption spectra of MB in water after irradiation under a 300 W Xe lamp in the presence of **2**; (b) The degradation ratios of MB in water in the presence of **1-5** under a 300 W Xe lamp irradiation for 17 min.

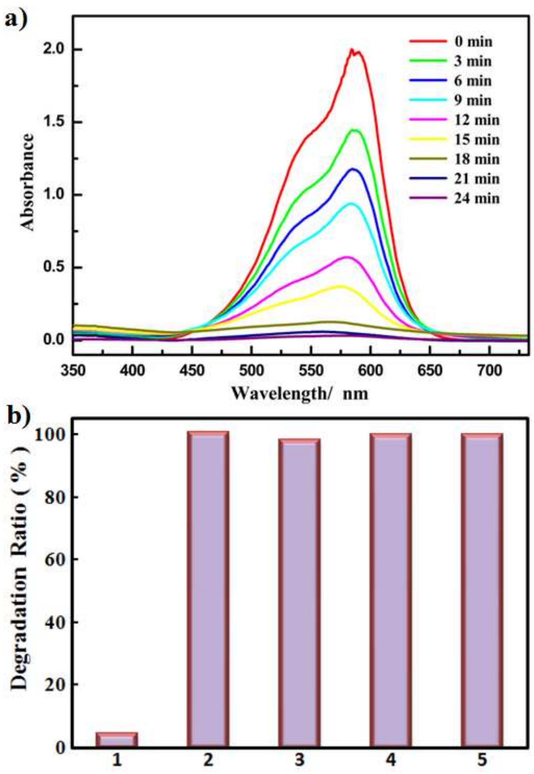

Fig. 7 (a) UV-Vis absorption spectra of CV in water after irradiation under a 300 W Xe lamp in the presence of **2**; (b) The degradation ratios of CV in water in the presence of **1-5** under a 300 W Xe lamp irradiation for 24 min.

Dalton Transactions Accepted Manuscript

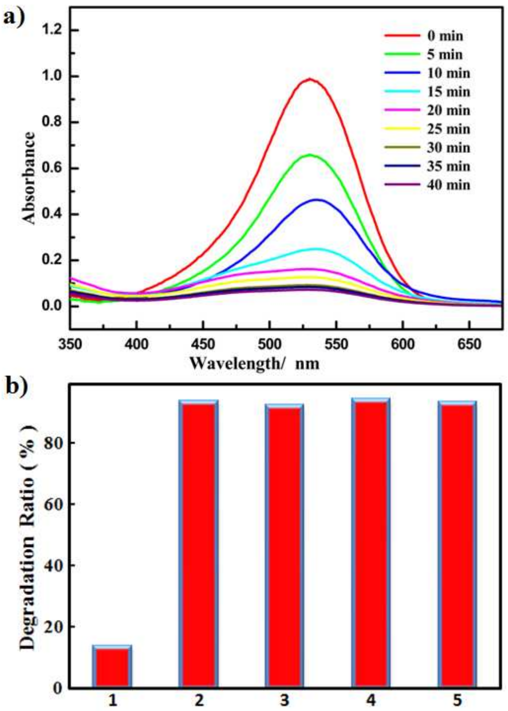

Fig. 8 UV-Vis absorption spectra of NR after irradiation under a 300 W Xe lamp in the presence of **2**; (b) The degraded ratios of NR in water in the presence of **1-5** under a 300W Xe lamp irradiation for 40 min.

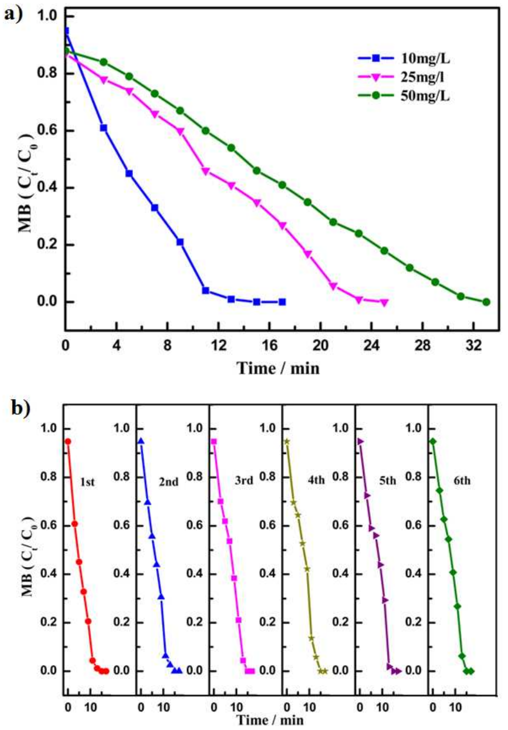

Fig. 9 (a) Photolysis of MB dye with different initial concentrations in water catalyzed by **2**; (b) Recycling photodegradation of MB dye in water catalyzed by **2** under a 300W Xe lamp irradiation.

As shown in Fig. 9a, when the initial concentration of MB dye was increased from 10.0 mg L^{-1} to 50 mg L^{-1}, the MB dye can also be completely photolyzed by **2** under the same conditions. After the photolysis reaction proceeded for 7 min, the solid catalyst was removed by centrifugation. The plasma was irradiated under a 300 W Xe lamp under otherwise identical conditions. UV-Vis absorption spectroscopy analysis demonstrates that the photolysis reaction did not proceed anymore, which proved the heterogeneously catalytic property of **2** in nature (Fig. S16). PXRD pattern of the recovered solid suggests that the structural integrity of the catalyst was maintained during catalysis. Furthermore, catalyst **2** can be simply recovered by centrifugation, thoroughly washed with water, and subsequently used in successive runs for six cycles without loss of catalytic efficiency (Fig. 9b).

Conclusions

In summary, immobilizing both zwitterion and POM moieties into the frameworks of porous hybrid materials represents a promising field for highly efficient photocatalysis. Considering that the two species have high affinity, we have developed an effective strategy to successfully synthesize a series of novel anionic zwitterion-POM hybrids **2-5**, in which the POM units act as templates and photoactive moieties. These hybrid materials combine two kinds of very different functional moieties in the pore surfaces, exhibiting remarkable efficiency on selective scavenging and photolysis of cationic dyes from polluted water, in which up to 10% dye uptake and quantitative photolysis of dye have been realized. This work represents a great progress for the synthesis of porous hybrid materials for practical applications in different fields.

Acknowledgements

We are grateful for the financial support of the National Natural Science Foundation of China (Grant No. 21373180), and the research fund of Key Laboratory for Advanced Technology in Environmental Protection of Jiangsu Province (Grant No. AE201301).

Notes and references

[a] *Center for Chemistry of High-Performance and Novel Materials, Department of Chemistry, Zhejiang University, Hangzhou, 310027, P.R. China; E-mail: cdwu@zju.edu.cn*

† Electronic Supplementary Information (ESI) available: Additional data, figures and tables. CCDC 1048166 (**1**), 1048168-1048171 (**2-5**). See DOI: 10.1039/b000000x/

1 (a) C. Wang, T. Zhang and W. Lin, *Chem. Rev.*, 2012, **112**, 1084; (b) J. Yu, Y. Cui, C. Wu, Y. Yang, Z. Wang, M. O'Keeffe, B. Chen and G. Qian, *Angew. Chem., Int. Ed.*, 2012, **51**, 10542; (c) L. K. Myers, C. Langhoff and M. E. Thompson, *J. Am. Chem. Soc.*, 1992, **114**, 7560; (d) G.-Q. Kong and C.-D. Wu, *CrystEngComm*, 2012, **14**, 847.

2 (a) L. Ma, C. Abney and W. Lin, *Chem. Soc. Rev.*, 2009, **38**, 1248; (b) J. Lee, O. K. Farha, J. Roberts, K. A. Scheidt, S. T. Nguyen and J. T. Hupp, *Chem. Soc. Rev.*, 2009, **38**, 1450; (c) A. Corma, H. García and F. X. Llabrés i Xamena, *Chem. Rev.*, 2010, **110**, 4606; (d) Y. Liu, W. M. Xuan and Y. Cui, *Adv. Mater.*, 2010, **22**, 4112; (e) M. Yoon, R. Srirambalaji and K. Kim, *Chem. Rev.*, 2012, **112**, 1196; (f) S. Ou and C.-D. Wu, *Inorg. Chem. Front.*, 2014, **1**, 721; (g) J. Liu, L. Chen, H. Cui, J. Zhang, L. Zhang and C.-Y. Su, *Chem. Soc. Rev.*, 2014, **43**, 6011; (h) M. Zhao, S. Ou and C.-D. Wu, *Acc. Chem. Res.*, 2014, **47**, 1199.

Dalton Transactions Accepted Manuscript

This journal is © The Royal Society of Chemistry [year]

3 (a) Z. Hu, B. J. Deibert and J. Li, *Chem. Soc. Rev.*, 2014, **43**, 5815; (b) Y. Cui, Y. Yue, G. Qian, and B. Chen, *Chem. Rev.*, 2012, **112**, 1126.

4 E. Coronado and G. Minguez Espallargas, *Chem. Soc. Rev.*, 2013, **42**, 1525.

5 (a) K. Sumida, D. L. Rogow, J. A. Mason, T. M. McDonald, E. D. Bloch, Z. R. Herm, T.-H. Bae and J. R. Long, *Chem. Rev.*, 2012, **112**, 724; (b) J.-R. Li, J. Sculley and H.-C. Zhou, *Chem. Rev.*, 2012, **112**, 869; (c) H. Wu, Q. Gong, D. H. Olson and J. Li, *Chem. Rev.*, 2012, **112**, 836.

6 (a) J.-R. Li, R. J. Kuppler and H.-C. Zhou, *Chem. Soc. Rev.*, 2009, **38**, 1477; (b) M. P. Suh, H. J. Park, T. K. Prasad and D.-W. Lim, *Chem. Rev.*, 2012, **112**, 782.

7 (a) Y. Takashima, V. M. Martínez, S. Furukawa, M. Kondo, S. Shimomura, H. Uehara, M. Nakahama, K. Sugimoto and S. Kitagawa, *Nat. Commun.*, 2011, **2**, 168; (b) M.-J. Dong, M. Zhao, S. Ou, C. Zou and C.-D. Wu, *Angew. Chem., Int. Ed.*, 2014, **53**, 1575; (c) A. Lan, K. Li, H. Wu, D. H. Olson, T. J. Emge, W. Ki, M. Hong and J. Li, *Angew. Chem., Int. Ed.*, 2009, **48**, 2334; (d) H.-L. Jiang, Y. Tatsu, Z.-H. Lu and Q. Xu, *J. Am. Chem. Soc.*, 2010, **132**, 5586; (e) M.-S. Wang, S.-P. Guo, Y. Li, L.-Z. Cai, J.-P. Zou, G. Xu, W.-W. Zhou, F.-K. Zheng and G.-C. Guo, *J. Am. Chem. Soc.*, 2009, **131**, 13572; (f) C. Zhan, S. Ou, C. Zou, M. Zhao and C.-D. Wu, *Anal. Chem.,* 2014, **86**, 6648.

8 (a) P. Wasserscheid and W. Keim, *Angew. Chem., Int. Ed.*, 2000, **39**, 3772 ; (b) J. Dupont, R. F. de Souza and P. A. Z. Suarez, *Chem. Rev.*, 2002, **102**, 3667; (c) J. Huang, T. Jiang, H. Gao, B. Han, Z. Liu, W. Wu, Y. Chang and G. Zhao, *Angew. Chem., Int. Ed.*, 2004, **43**, 1397; (d) W. Miao and T. H. Chan, *Acc. Chem. Res.*, 2006, **39**, 897.

9 (a) G.-Q. Kong, S. Ou, C. Zou and C.-D. Wu, *J. Am. Chem. Soc.*, 2012, **134**, 19851; (b) G.-Q. Kong, X. Xu, C. Zou and C.-D. Wu, *Chem.Commun.*, 2011, **47**, 11005; (c) G.-Q. Kong and C.-D. Wu, *Cryst. Growth Des.*, 2010, **10**, 4590; (d) M. B. Lalonde, R. B. Getman, J. Y. Lee, J. M. Roberts, A. A. Sarjeant, K. A. Scheidt, P. A. Georgiev, J. P. Embs, J. Eckert, O. K. Farha, R. Q. Snurr and J. T. Hupp, *CrystEngComm*, 2013, **15**, 9408; (e) X.-W. Wang, L. Han, T.-J. Cai, Y.-Q. Zheng, J.-Z. Chen and Q. Deng, *Cryst. Growth Des.*, 2007, **6**, 1027; (f) X. Li, X. Guo, X. Weng and S. Lin, *CrystEngComm*, 2012, **14**, 1412.

10 (a) C. L. Hill, *Chem. Rev.*, 1998, **98**, 1; (b) D.-L. Long, R. Tsunashima and L. Cronin, *Angew. Chem., Int. Ed.*, 2010, **49**, 1736; (c) H. Lv, Y. V. Geletii, C. Zhao, J. W. Vickers, G. Zhu, Z. Luo, J. Song, T. Lian, D. G. Musaev and C. L. Hill, *Chem. Soc. Rev.*, 2012, **41**, 7572; (d) S.-T. Zheng and G.-Y. Yang, *Chem. Soc. Rev.*, 2012, **41**, 7623; (e) A. Dolbecq, E. Dumas, C. R. Mayer and P. Mialane, *Chem. Rev.*, 2010, **110**, 6009; (f) H. N. Miras, L. Vilà-Nadal and L. Cronin, *Chem. Soc. Rev.*, 2014, **43**, 5679; (g) R. Yu, X.-F. Kuang, X.-Y. Wu, C.-Z. Lu and J. P. Donahue, *Coord. Chem. Rev.*, 2009, **253**, 2872; (h) M. Mirzaei, H. Eshtiagh-Hosseini, M. Alipour and A. Frontera, *Coord. Chem. Rev.*, 2014, **275**, 1.

11 (a) T. Li, Q. Li, J. Yan, and F. Li, *Dalton Trans.*, 2014, **43**, 9061; (b) S. Bala, S. Bhattacharya, A. Goswami, A. Adhikary, S. Konar and R. Mondal, *Cryst. Growth Des.*, 2014, **14**, 6391; (c) N. Lua, Y. Zhao, H. Liu, Y. Guo, X. Yuan, H. Xu, H. Peng and H. Qin, *J. Hazard. Mater.*, 2012, **199**, 1; (d) P. Ngaotrakanwiwat, T. Tatsuma, S. Saitoh, Y. Ohkob and A. Fujishim, *Phys. Chem. Chem. Phys.*, 2003, **5**, 3234; (e) D. A. Friesen, L. Morello, J. V. Headley and C. H. Langford, *J. Photochem. Photobiol. A*, 2000, **133**, 213.

12 (a) J. Song, Z. Luo, D. K. Britt, H. Furukawa, O. M. Yaghi, K. I. Hardcastle and C. L. Hill, *J. Am. Chem. Soc.*, 2011, **133**, 16839; (b) J. Song, Z. Luo, D. K. Britt, H. Furukawa, O. M. Yaghi, K. I. Hardcastle and C. L. Hill, *J. Am. Chem. Soc.*, 2011, **133**, 16839; (c) C. Zou, Z. J. Zhang, X. Xu, Q. H. Gong, J. Li and C.-D. Wu, *J. Am. Chem. Soc.*, 2012, **134**, 87; (d) F.-J. Ma, S.-X. Liu, C.-Y. Sun, D.-D. Liang, G.-J. Ren, F. Wei, Y.-G. Chen and Z.-M. Su, *J. Am. Chem. Soc.*, 2011, **133**, 4178; (e) Q.-X. Han, C. He, M. Zhao, B. Qi, J.-Y. Niu and C.-Y. Duan, *J. Am. Chem. Soc.*, 2013, **135**, 10186; (f) B. Nohra, H. E. Moll, L. M. R. Albelo, P. Mialane, J. Marrot, C. Mellot-Draznieks, M. O'Keeffe, R. N. Biboum, J. Lemaire, B. Keita, L. Nadjo and A. Dolbecq, *J. Am. Chem. Soc.*, 2011, **133**, 13363.

13 (a) S. Ahrens, E. Herdtweck, S. Goutal and T. Strassner, *Eur. J. Inorg. Chem.*, **2006**, 1268; (b) J. Liu, J. Chen, J. Zhao, Y. Zhao, L. Li and H. Zhang, *Synthesis*, **2003**, 2661.

14 Oxford Diffraction Ltd. CrysAlisPro, Version 1.171.33.56, **2010**.

15 G. M. Sheldrick, *Program for Structure Refinement*: University of Göttingen, Germany, **1997**.

16 A. L. Spek, Single-crystal structure validation with the program PLATON. *J. Appl. Cryst.*, 2003, **36**, 7.

17 K. Nakajima, K. Eda, and S. Himeno, *Inorg. Chem.*, 2010, **49**, 5212.

18 A. L. Spek, *PLATON*, *a multipurpose crystallographic tool*, Utrecht University, Utrecht, the Netherlands, 2009.

19 J. R. Lakowicz, *Principles of Fluorescence Spectroscopy*, 3rd ed., Springer: Berlin, **2006**.

20 (a) D. Ravelli, D. Dondi, M. Fagnoni and A. Albini, *Chem. Soc. Rev.,* 2009, **38**, 1999; (b) L.-L. Wen, L. Zhou, B.-G. Zhang, X.-G. Meng, H. Qua and D.-F. Li, *J. Mater. Chem.,* 2012, **22**, 22603; (c) S. Zhang, L. Han, L. N. Li, J. Cheng, D. Yuan and J. Luo, *Cryst. Growth Des.,* 2013, **13**, 5466; (d) R. Li, X.-Q. Ren, H.-W. Ma, X. Feng, Z.-G. Lin, X.-G. Li, C. W. Hu and B. Wang, *J. Mater. Chem. A,* 2014, **2**, 5724; (e) W.-Q. Kan, B. Liu, J. Yang, Y.-Y. Liu and J.-F. Ma, *Cryst. Growth Des.,* 2012, **12**, 2288; (f) Y. Hu, F. Luo and F.-F. Dong, *Chem. Commun.*, 2011, **47**, 761; (g) Y.-Q. Chen, S.-J. Liu, Y.-W. Li, G.-R. Li, K.-H. He, Y.-K. Qu, T.-L. Hu and X.-H. Bu, *Cryst. Growth Des.*, 2012, **12**, 5426; (h) H. Yang, X.-W. He, F. Wang, Y. Kang and J. Zhang, *J. Mater. Chem.,* 2012, **22**, 21849; (i) M. C. Das, H. Xu, Z. Wang, G. Srinivas, W. Zhou, Y. Yue, V. N. Nesterov, G. Qian and B. Chen, *Chem. Commun.,* 2011, **47**, 11715; (j) Y.-Q. Chen, G.-R. Li, Y.-K. Qu, Y.-H. Zhang, K.-H. He, Q. Gao and X.-H. Bu, *Cryst. Growth Des.,* 2013, **13**, 901; (k) B. Liu, Z.-T. Yu, J. Yang, H. Wu, Y.-Y. Liu and J.-F. Ma, *Inorg. Chem.*, 2011, **50**, 8967.

21 X. P. Lin, T. Huang and F. Q. Huang, *J. Phys. Chem. B*, 2006, **110**, 24629.

Dalton Transactions Accepted Manuscript

Graphical Abstract

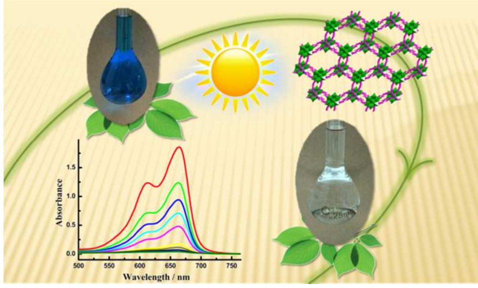

An effective strategy to immobilize both zwitterion and POM moieties into porous hybrid materials was developed, which demonstrate remarkable efficiency on selective scavenging and photolysis of cationic dyes from polluted water.

Dalton Transactions Accepted Manuscript